

Effect of pre-existing microstructural defects on elastic and fracture properties of composites

Ponnusami, Sathiskumar A.; Pathan, Mehtab V.; Erice, Borja; Petrinic, Nik

Publication date

2017

Document Version

Final published version

Published in

21st International Conference on Composite Materials, ICCM 2017

Citation (APA)

Ponnusami, S. A., Pathan, M. V., Erice, B., & Petrinic, N. (2017). Effect of pre-existing microstructural defects on elastic and fracture properties of composites. In *21st International Conference on Composite Materials, ICCM 2017* (Vol. 2017-August). International Committee on Composite Materials.

Important note

To cite this publication, please use the final published version (if applicable). Please check the document version above.

Copyright

Other than for strictly personal use, it is not permitted to download, forward or distribute the text or part of it, without the consent of the author(s) and/or copyright holder(s), unless the work is under an open content license such as Creative Commons.

Takedown policy

Please contact us and provide details if you believe this document breaches copyrights. We will remove access to the work immediately and investigate your claim.

EFFECT OF PRE-EXISTING MICROSTRUCTURAL DEFECTS ON ELASTIC AND FRACTURE PROPERTIES OF COMPOSITES

Sathiskumar A. Ponnusami^{1,2}, Mehtab V. Pathan^{1,3}, Borja Erice¹ and Nik Petrinic¹

¹ Impact Engineering Laboratory, Solid Mechanics and Materials Engineering Group, Department of Engineering Science, University of Oxford, Oxford, United Kingdom.

² Dept. of Aerospace Structures and Materials, Delft University of Technology, Delft, Netherlands.

³ Dept. of Aeronautics, Imperial College London, United Kingdom.

Email: sathis.ponnusami@eng.ox.ac.uk , mehtab.pathan@eng.ox.ac.uk , borja.eric@eng.ox.ac.uk and nik.petrinic@eng.ox.ac.uk

Keywords: Fiber-reinforced composites, Microstructural defects, Cohesive elements, Pores and interface cracks, Elastic and fracture properties

ABSTRACT

The objective of this research is to explore the effect of microstructural defects on the mechanical properties of fiber reinforced composites. In particular, two kinds of defects are considered in the study, namely, matrix pores and interface precracks. Three-dimensional (3-D) finite element analyses are conducted on Representative Volume Elements (RVE) to predict the effective elastic properties of the transversely isotropic unidirectional composite with a random distribution of the pore defects and the results are reported. With regards to fracture properties, cohesive zone-based two-dimensional (2-D) finite elements are employed to simulate fracture in the microstructure, where the cohesive elements are embedded throughout the FE mesh to simulate arbitrary crack initiation and propagation. The results of the simulations are reported in terms of the fracture pattern and quantified using the effective stress-strain response for various volume and area fractions of matrix pores and interface cracks respectively. It is shown that the presence of defects has a noticeable influence on the elastic properties, but severely influences the fracture properties of the composite.

1 INTRODUCTION

Composite materials are being used extensively in the aerospace industry due to their superior specific mechanical properties. However, compared to the conventional metallic materials, their heterogeneity and complex microstructure make it rather difficult to predict their mechanical properties, i.e., elastic moduli and fracture strength and toughness. With the above factors, added with the nature of composite manufacturing techniques, the occurrence or presence of defects becomes an inherent characteristic of the composite materials. The type and distribution of the defects depend on several factors, however, two distinct defects can be identified from a typical composite microstructure as shown in Fig. 1, namely pores and pre-existing cracks.

Not many attempts are made in the literature to address the issue of these defects [1-5] and only a few studies exist on explicit modelling of the distribution of defects and their influence on the mechanical properties of composites. For instance, in the reference [3], the effect of interface defects is analyzed using an elastoplastic damage model in a metal matrix composite. More recently, a continuum damage model-based approach is employed to quantify the effect of matrix pores in an alumina fiber reinforced aluminum matrix composite [4]. The scope for research in this field is broad and would yield practical insights on the effects of manufacturing induced defects on composite behavior. From this perspective, it is the objective of this research to investigate and quantify the effect of pre-existing defects on the composite elastic and fracture properties.

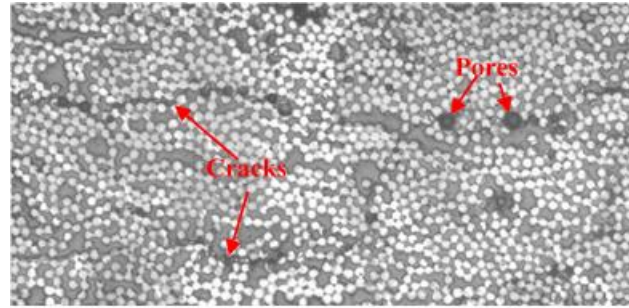


Figure 1: Micrograph of a fiber composite cross-section showing presence of pores and pre-existing micro-cracks

2 MODELLING APPROACH

The goal of present study is to analyze the effect of the microstructural defects on both elastic and fracture properties of unidirectional fiber composites using high-fidelity numerical models. Accordingly, two major sections as listed below address the above objectives.

- For elastic properties, three-dimensional Representative Volume Elements (RVE)-based homogenization with random distributions of pores is utilized.
- For fracture properties, two-dimensional RVE-based finite element analyses using cohesive elements are conducted.

For elastic properties: To represent realistic microstructure, three-dimensional volume elements and their finite element mesh with random arrangements of fibers are generated as shown in Fig.2. The microstructure generation is based on a constrained optimization algorithm adopted from [6], which has been shown to generate uncorrelated microstructures of FRPs. As mentioned previously, two different types of defects, the matrix pores and the interface cracks are included in the microstructure with varying volume fractions for the pores and equivalent surface area fraction for the interface cracks. Again, the distribution of these pores and interface cracks are random in nature generated using Random Sequential Adsorption (RSA) algorithm. Periodic boundary conditions are enforced on the RVE. In the current study, a square RVE of side length $L=24 \cdot R_f$ (R_f is the fiber radius) is analyzed following the previous work of the authors for which the convergence of elastic properties is ensured [6]. Modelling of the pores in the 3-D FE model is done implicitly by assigning significantly reduced stiffness properties to the existing finite elements in the pore regions. The 3-D models were meshed using a combination of tetrahedral (C3D6) and hexahedral (C3D8) solid elements with linear shape functions in Abaqus.

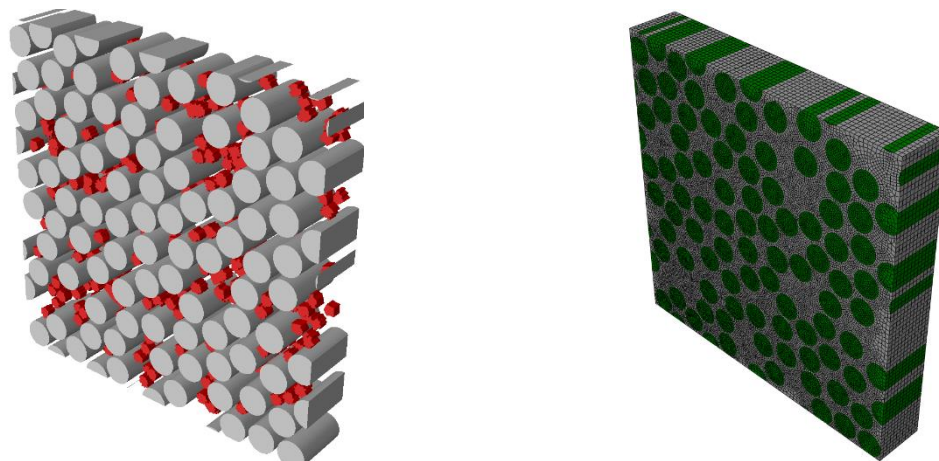


Figure 2: (a) A 3-D RVE with pores (highlighted by red color) and (b) the FE mesh (pores not highlighted).

For fracture properties: As for the fracture properties are concerned, a three-dimensional FE approach would be computationally expensive and not feasible for an extensive parametric study. Hence, a two-dimensional RVE is considered with a random distribution of the fibers and the defects. Plane strain conditions are assumed. A very fine and random/unstructured 2-D mesh is generated on the volume element with three-noded elements using Gmsh tool. A python script is then used to insert cohesive elements throughout the FE mesh, i.e. in the matrix, the fiber and on the interface; thereby facilitating the study of all three types of fracture mechanisms, namely fiber fracture, interface debonding and matrix cracking, when needed. Further, such an approach enables arbitrary crack initiation and propagation in the analysis according to the prescribed boundary conditions. However, finer mesh and randomness in the mesh are critical requirements for such fracture simulations to minimize the mesh dependency of the resulting crack path, refer [2]. In the current study, the ratio of element size and the fiber radius is taken as 15, resulting in a fine mesh, allowing for arbitrary crack growth, see Fig.3 (b). Periodic boundary conditions are prescribed on the surface of the RVE. As cohesive elements are on the boundaries as well, care is taken to identify the appropriate node pairs on the boundary faces enabling crack propagation and opening of the boundary faces [7].

A bilinear mixed-mode traction-separation constitutive relation [2] is used for the cohesive elements with distinct fracture properties for the matrix, the fiber and the interface. Such a cohesive law is characterized by three parameters, namely, cohesive strength, fracture energy and cohesive stiffness. Among them, cohesive stiffness is a numerical parameter, which is set artificially large to prevent adding artificial compliance to the structure, prior to failure initiation. A high value is deemed necessary especially for a fiber mesh with cohesive elements present throughout the mesh. The other two parameters, the strength and the energy correspond to the properties of the material phase under consideration. To allow for mode-mixity, relevant for the interface behavior, a power law is used. Abaqus/Standard is used as the solver for the analyses with COH2D4 cohesive elements to simulate fracture and CPE3 2-D solid elements to model the bulk constitutive behavior.

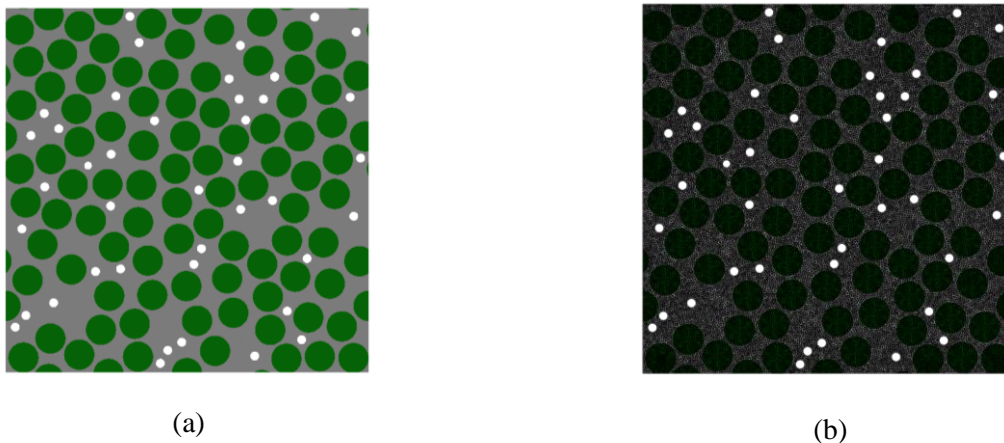


Figure 3: Two-dimensional RVE with random distribution of fibers and matrix pores, (a) Geometrical RVE; (b) Finite element mesh with embedded cohesive elements throughout the mesh.

3 ELASTIC PROPERTIES: EFFECT OF PORES

For predicting the effective elastic properties, conventional homogenization procedure is adopted with periodic boundary conditions applied over the RVE. As far as the elastic properties are concerned, linear elastic analyses are conducted in which evolution of pre-existing defects are not allowed. Both the fiber and matrix are assumed to be linear elastic and isotropic solids and their mechanical properties are taken to be representative of a glass fiber-epoxy composite. The material properties of the fiber and the matrix used in the analysis and the geometrical details of the model are as follows: Young's modulus of the fiber and the matrix, respectively, $E_f= 50$ GPa, $E_m= 3$ GPa; Poisson's ratio of the fiber and the matrix, $\nu_f=0.2$ and $\nu_m = 0.38$ respectively; fibre radius (R_f) = 7 μm , square RVE of side length $L=24^*$

R_f and thickness $t = 4 * R_f$. In order to assess the effect of pore volume fraction (v_p) on the mechanical response of FRPs, the fiber volume fraction (v_f) is fixed to a value of 0.5. As discussed before, each pore is assumed to be approximately spherical with radius equal to 15% of the fiber radius. These pores are implicitly modelled by assigning the elements within the pore region, artificially lower values of Young's modulus (ratio of modulus of the pore to that of the matrix is taken as equal to $10e-6$). Three different pore volume fractions, v_p , are considered: 0.02, 0.04 and 0.06, i.e., 2%, 4% and 6%. A quasi-static analysis is conducted in multiple steps for different loading conditions, namely, tension and shear in longitudinal (fiber) and transverse directions. This series of analysis would result in the required transversely isotropic tensor governing the effective elastic behavior of the composite material with five independent material constants *viz.*, Young's modulus along the fiber and transverse directions, E_1 and E_2 , Poisson's ratio, ν_{12} , in-plane shear modulus, G_{12} and out-of-plane shear modulus, G_{23} . A mesh convergence study was performed to ensure mesh-independent results.

The results of the simulations are summarized in Table 1, showing respectively the above five effective material constants. It is very clear that the Young's modulus, E_1 is very weakly influenced by the presence of pores (reduced by less than 1% for a pore volume fraction, $v_p = 0.06$ compared to baseline model with no pores), an obvious result as it is a fiber-dominated property. On the other hand, one can observe a rather considerable reduction of the matrix-dominated transverse Young's modulus, E_2 . For instance, for the pore volume fraction, $v_p = 0.06$, the transverse Young's modulus, E_2 , is decreased by 15% with respect to the transverse modulus of a non-porous composite of same fiber volume fraction. Similarly, the in-plane shear modulus G_{12} and out-of-plane shear modulus, G_{23} are reduced by 11.6% and 12.1% respectively. Again, it is observed that the matrix-dominated properties are reduced considerably with the introduction of pores. Similarly, the Poisson's ratio, ν_{12} is reduced by 9.1% as compared with the pristine, non-porous composite.

Pore, v_p	E_1 [GPa]	E_2 [GPa]	G_{12} [GPa]	G_{23} [GPa]	ν_{12} [-]
0	26.500	8.746	3.095	3.06	0.2776
0.02	26.440	8.283	2.980	2.94	0.2716
0.04	26.380	7.861	2.858	2.826	0.2659
0.06	26.320	7.406	2.734	2.688	0.2607

Table 1: Effect of pore volume fraction on elastic constants of the composite.

4 FRACTURE PROPERTIES

As discussed before, cohesive elements are inserted all along the element boundaries in order to facilitate arbitrary crack initiation region and propagation direction. For the purpose of simplicity and to have a specific focus on the effect of defects (pores and cracks), only tensile (or global Mode-I) loading conditions are considered for the analyses. From the analyses results, the influence of defects on the crack pattern and the effective composite strength are discussed. The elastic properties of the fiber and the matrix correspond to the same values as used before in the previous section. To limit the number of simulations, only one fiber volume fraction is considered and is taken equal to 0.5. Again, a quasi-static analysis is conducted with prescribed periodic boundary conditions corresponding to global Mode-I tensile loading. The fracture strength and the fracture energy of the matrix are taken to be 100 MPa and 0.1 N/mm respectively, while the strength of the fiber is taken as 2 GPa, making them 20 times stronger than the matrix, which is a realistic assumption. The interface between the fiber and matrix is assumed to be perfectly bonded. This is achieved by assigning a very high value for the interface fracture

properties, which in this case is taken as 10 times higher than the matrix fracture properties. Such an assumption is not necessary *per se*, but imposed in order to keep the number of variables minimum and to focus primarily on the effect of the defects on the composite strength.

4.1 EFFECT OF PORE DEFECTS

Three pore volume fractions, $v_p = 2\%$, 4% and 6% , are considered in the analyses, results of which are summarized in Fig. 4 and 5. In particular, the resulting crack path and the average stress-strain response are reported in the Figures. From Fig.4 (a) corresponding to a microstructure without pores, it can be observed the fracture is driven by matrix cracking, in which the crack follows a resin rich path in the microstructure. In other words, the evolving microcracks avoid the stiffer and stronger fibers, resulting in less interference with the fibers. On the other hand, in presence of pores in the microstructure, the cracking mechanism is strongly influenced by their presence as evident from Fig. 4 (b). In the case without pores, the microcracks initiate in the matrix due to the stress concentrations induced by the presence of fibers. Conversely, in the presence of pores, the crack initiation is also majorly triggered by stress concentration induced by the pores, in addition to the stress amplifications due to the presence of the fibers. From examining the resulting crack paths in the two cases, it can be observed that a more torturous fracture pattern is resulted with the introduction of pores.

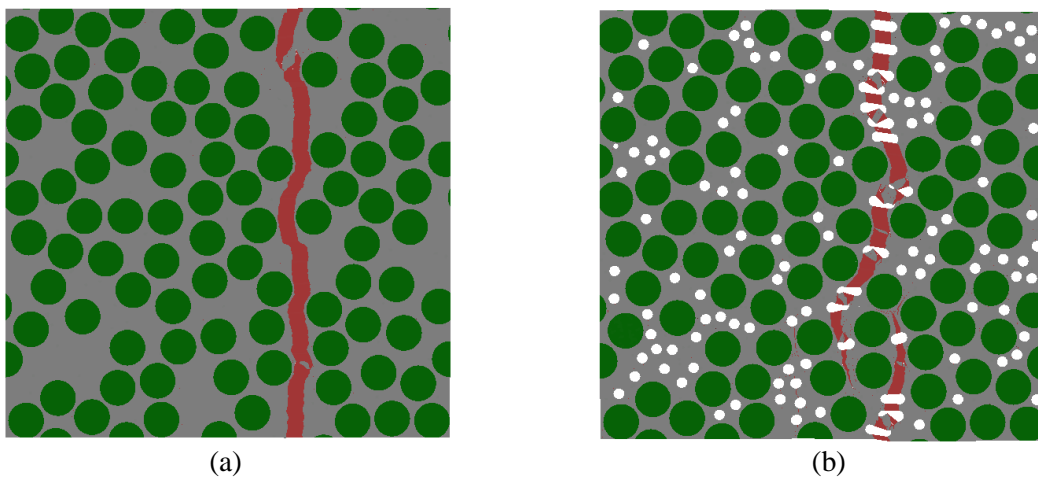


Figure 4: Simulated crack paths in the microstructure with fixed fibre volume fraction $v_f=50\%$, (a) no pores; (b) pore volume fraction, $v_p=6\%$

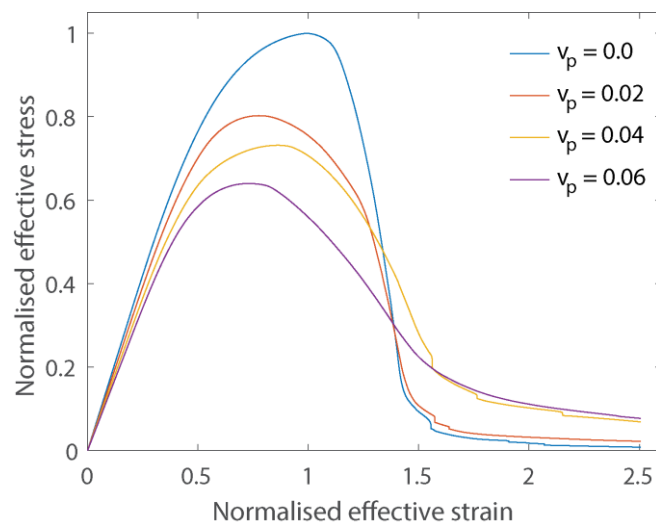


Figure 5: Variation of the effective stress-strain response of the GFRP composite with pore volume fraction for the case of fiber volume fraction = 50%.

The normalized stress-strain response of the composite corresponding to different pore volume fractions is reported in Fig.5. The stress and the strain are obtained, respectively, by normalizing the reaction force with the cross-sectional area over which the displacements are prescribed and the relative displacement (or extension) with the length of the RVE. The effective stress is normalized by fracture strength of the composite without the pores and the effective strain is normalized by the strain corresponding to the peak stress (strength) of the composite without the pores. From the results, it is very clear that the presence of pores significantly affects the fracture strength of the composite. For instance, a mere 2 % volume fraction of the pores reduces the composite strength by approximately 20 %. With the increase in the pore volume fraction, the strength reduces further and falls to 60% of the non-porous composite strength. Needless to mention, the presence of pores affects the initial slope, which corresponds to the transverse Young's modulus of the composite, as discussed in section 2. From these 2-D simulations, it is found that, for a pore volume fraction of 6%, the elastic modulus in the transverse direction is reduced by 18% as compared with the non-porous composite. This result correlates reasonably well with the 3-D simulations, which are much more accurate due to obvious reasons. Another general feature to note is with regards to the post-peak response, in which a pseudo-ductility is induced by the pores, in other words, the presence of the pores leads to a smoother fracture process in an otherwise relatively brittle fracture in the composite.

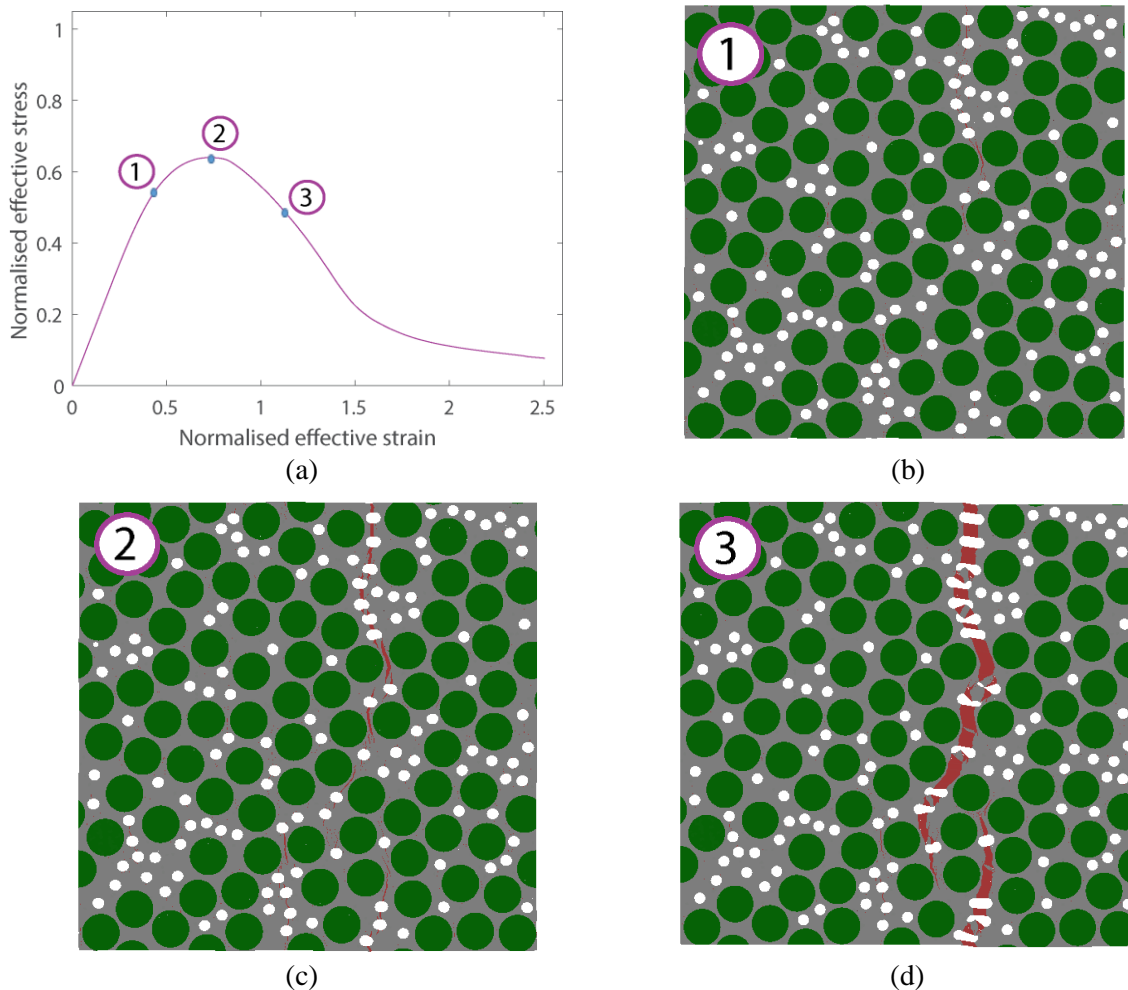


Figure 6: Evolution of crack path/pattern in the presence of pores. (a) Stress-strain curve with pore volume fraction of $v_p=0.04$; (b), (c) and (d) shows the crack evolution.

To have a further understanding on the effect of pores, a sequence of fracture events or evolution in the microstructure with pores is reported in Fig.6. In principle, upon loading the RVE, several microcracks initiate in the pores and further propagate to coalesce to form a macro-crack as observed from Fig. 6 (a) to (c). Note that the peak stress or the strength does not correspond to the crack initiation in the microstructure. In other words, the composite strength or the peak stress (point 2 in Fig.6 (a)) is not governed by the initiation of a crack within the microstructure, rather the effective stress in the composite drops only after several microcracks appear, refer point 2 in Fig.6 (a) and (c).

4.2 EFFECT OF INTERFACE FLAWS:

To examine the effect of interface defects (precracks), three different equivalent area fractions, $v_i=0.05, 0.1$ and 0.15 , of the pre-existing interface cracks are considered. The equivalent area fraction, v_i , of the interface defects is defined as the ratio of the precracked interface area to the total interface area. The distribution of the defects is random in nature with a restriction on the maximum defect area per fiber/matrix interface. The implementation or incorporation of the interface defects is done as follows. Once the location, size and distribution of the interface flaws are decided, the interface cohesive elements in the corresponding region are assigned very low values of the strength and fracture energy, approximately equal to 100 times lower than that of the matrix. By doing this, the flawed interface elements would fail immediately after the application of very low load levels in the very initial stage of the analysis, allowing us to model them as interface defects during rest of the loading process.

As done with the RVEs with pores, a global Mode-I loading is prescribed using periodic boundary conditions. The results of the simulations are reported in the Fig.7, in terms of resulting crack paths and the average stress-strain response. In Fig.7, the highlighted bright red parts of the cracked region correspond to the preexisting interface defects, while dark red colored parts of the remaining crack path are the evolved new matrix cracks. Parts of the fiber/matrix interfaces highlighted in red in the rest of the RVE are the initial interface flaws.

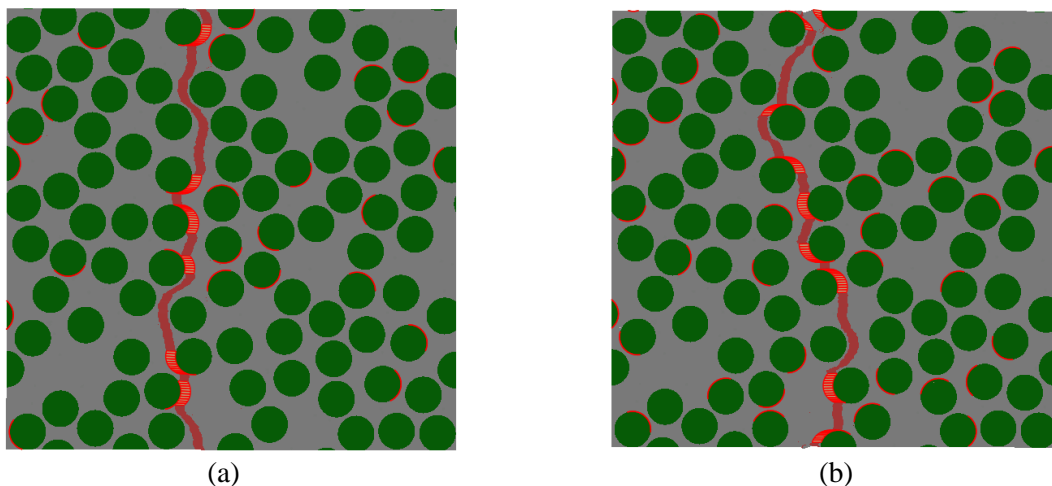


Figure 7: Simulated crack paths with interface defect area fraction, (a) $v_i=0.1$ and (b) $v_i=0.15$.

From the crack paths, it can be observed that the presence of interface defects alters the fracture pattern significantly. As compared with the no defect case in Fig.4(a), the presence of interface defects facilitates crack initiation from the interface defects, leading to varying fracture patterns. It can be observed, for instance in the cases (a) and (b) in Fig.7, a crack path different from the one without interface defect (Fig.4(a)) is resulted, which in turn is the result of coalescence of microcracks from the existing interface defects. To explain further, Fig.8 reveals the crack evolution in the microstructural RVE in the presence of interface defects. Upon initial loading, the interface flaws which are locally loaded in opening mode induce stress concentrations in its vicinity as seen in Fig.8(a). With further

deformation, multiple new micro cracks emanate from the existing interface defects (or crack) as observed in Fig. 8(b). Subsequently, some of the energetically favored microcracks grow further into the matrix and coalesce with each other as seen in Fig. 8(c), ultimately resulting in a major crack and hence the failure of the RVE, refer Fig. 8(d).

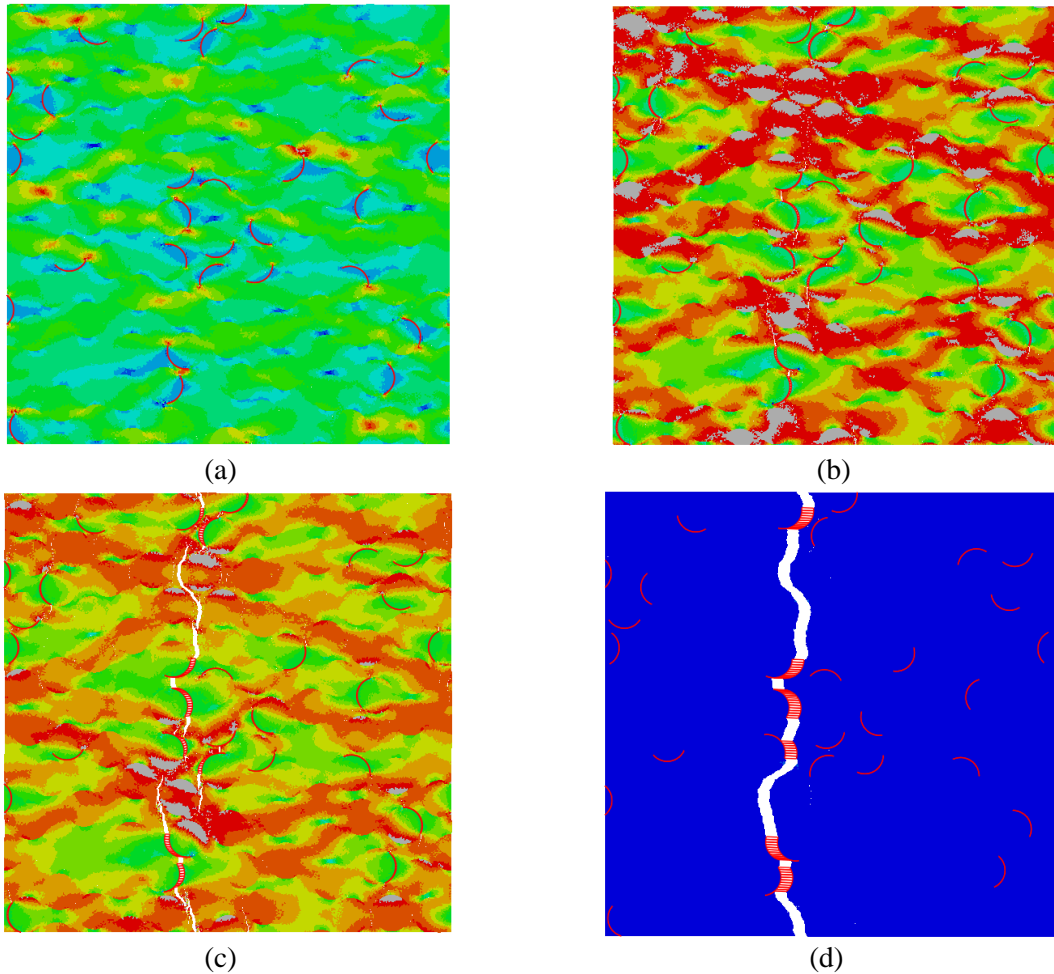


Figure 8: Crack evolution in the microstructure with interface defects, (a) initial loading phase, where stress concentrations in the vicinity of interface defects (under local tension) are observed; (b) upon increasing the loading, microcracks originate from the interface defects; (c) the microcracks then propagate and coalesce with each other; (d) in the end, a major crack forms, resulting in complete failure of the RVE. The defect area fraction in the considered case is equal to $v_i=0.1$.

To quantify the effect of the interface defects on the composite strength, the effective stress-strain response of the RVE is plotted for three area fractions of the defects. The stress and the strain are normalized as done in the case of pores. From the Fig. 9, it is found that presence of interface flaws has a detrimental effect on the composite strength, which reduces monotonically with increase in the area fraction of the defects. From the results, for the defect area fraction equal to 15%, the composite strength reduces as much as 55% w.r.t the strength of the composite RVE without defects. Further, it is observed that the strain required to reach the peak stress decreases with increase in the defect area fraction.

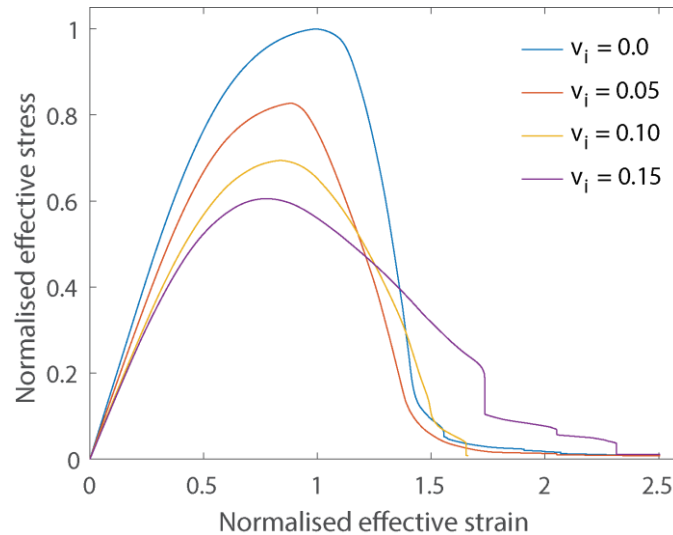


Figure 9: Effective stress-strain response of the composite with and without interface defects with three equivalent area fractions of the defects.

5 CONCLUSIONS AND FURTHER RESEARCH

From the current study, the influence of microstructural defects on the crack pattern and the effective properties are examined. It is generally observed that the defects have a significant influence on the effective mechanical properties of the composite. The sensitivity of effective fracture properties to the presence of defects is much severe than that of the elastic properties. Some aspects which are chosen for further research are the stochastic nature of the defects, whereby multiple realizations of the RVE for each test case would lead to a more realistic representation of actual microstructure which is inherently stochastic. In the present study, the effect of interface defects on elastic properties is not dealt, which is part of our ongoing research. In addition, varying the matrix pore size and interface defect size per each fiber/matrix interface could reveal further information on their effects on both elastic and fracture properties of the composite, which will be dealt in further research. The results and the understanding of the effect of pre-existing defects on the composite behavior could open further research directions and offer practical insights in the design process.

REFERENCES

- [1] Huang H, Talreja R. *Effects of void geometry on elastic properties of unidirectional fiber reinforced composites*. Composites Science and Technology. 2005; 65(13):1964-1981.
- [2] Sathiskumar A Ponnusami, Sergio Turteltaub, Sybrand van der Zwaag. *Cohesive-zone modelling of crack nucleation and propagation in particulate composites*. Engineering Fracture Mechanics. 2015;149:170-90.
- [3] Pyo, S.H. and Lee, H.K., 2010. *An elastoplastic damage model for metal matrix composites considering progressive imperfect interface under transverse loading*. International Journal of Plasticity, 26(1), pp.25-41.
- [4] Ahmadian, H., Liang, B. and Soghrati, S., 2016. *Analyzing the impact of microstructural defects on the failure response of ceramic fiber reinforced aluminum composites*. International Journal of Solids and Structures, 97, pp.43-55.
- [5] Soppa, E., Schmauder, S., Fischer, G., Brollo, J. and Weber, U., 2003. *Deformation and damage in Al/Al₂O₃*. Computational Materials Science, 28(3), pp.574-586.
- [6] Pathan M.V, Tagarielli V.L, Patsias S. *Numerical predictions of the anisotropic viscoelastic response of uni-directional fibre composites*. Composites Part A: Applied Science and Manufacturing. 2017;93:18-32.
- [7] Niels van Hoorn, Sergio Turteltaub, and Javad Fatemi. *Multiscale traction-separation relations for fiber-reinforced composites*, XXIV ICTAM, August 2016, Montreal, Canada.